First-principles calculations on the origin of ferroelectric and ferromagnetic properties in $La_{0.75}Bi_{0.25}CrO_3$

E. Martínez-Aguilar[1,2], H´Linh H´Mŏk[1,2], J. Ribas Ariño[3], J. M. Siqueiros Beltrones[2]

[1] Posgrado en Física de Materiales, Centro de Investigación Científica y de Educación Superior de Ensenada, Carretera Tijuana-Ensenada No. 3918, Zona Playitas, Ensenada 22860, B.C., México.
[2] Centro de Nanociencias y Nanotecnología, Universidad Nacional Autónoma de México, AP 14, Ensenada 22860, Baja California, México.
[3] Departament de Ciència de Materials i Química Física, Universitat de Barcelona, Martí i Franquès 1, 08028 Barcelona, Spain.

E-mail: espiridion.martinez.aguilar@gmail.com

Abstract

Despite the interesting properties of $La_{1-x}Bi_xCrO_3$, the origin of its multiferroic properties has not been yet established by calculations of first-principles, so in this work we report the comparison between structural, electronic, magnetic and ferroelectric properties of $LaCrO_3$ and $La_{0.75}Bi_{0.25}CrO_3$ through density functional theory (DFT) + formalism of Hubbard potential (U) and the Berry phase approach. At the same time we present a comparative analysis between the experimental results reported and the theoretical calculations in this work, in which we have determined that the $LaCrO_3$ is stable under a G-type antiferromagnetic configuration, while the $La_{0.75}Bi_{0.25}CrO_3$ is stable in ferromagnetic configuration. This is due to the decrease of the Cr-O-Cr angle which is strongly related with the high degree of covalence of the spin-up Cr-t_{2g} and O-2p orbitals in the Cr-O bonds. On the other hand, the ferroelectric character is attributed to the structural distortion induced by the lone pair of Bi in site A, which predicts a spontaneous polarization in $La_{0.75}Bi_{0.25}CrO_3$ of 60.31 $\mu C/cm^2$ in the direction [011], establishing with it the origin of the ferroelectric and magnetic properties observed experimentally for the $La_{1-x}Bi_xCrO_3$.

Keywords: first-principles calculations, DFT, ferromagnetism, ferroelectricity.

1. Introduction

Lanthanum chromite, $LaCrO_3$ (LCO), has an orthorhombic perovskite structure (with space group # 62 Pbnm). It has a G-type antiferromagnetic insulating ground state below its Néel temperature (320 K).[1] Its high electronic conductivity, low ionic conductivity and good chemical stability in both oxidizing and reducing environments at high temperatures have made LCO suitable for use as the interconnect material in solid-oxide fuel cells.[2-4] In recent investigations, the magnetic properties of LCO were found to be affected by the substitution of La with different cations like Ca, Sr, Nd under which a weak ferromagnetism appears.[5-7] No ferroelectric properties have been found in pure LCO.[4] However, the solid solution system of $La_{1-x}Bi_xCrO_3$ ($0.1 \leq x \leq 0.35$), prepared by conventional solid-state reaction method by J.I.L Chen et al., was found to display dielectric hysteresis loops at 77K. The spontaneous polarization increases with increasing Bi^{3+} content.[4] Moreover, H-Y. Guo et al. found that both ferroelectricity and magnetization are enhanced by the substitution of La^{3+} for Bi^{3+} in the $La_{1-x}Bi_xCrO_3$ solid solution.[8] This finding open up another application world for the $La_{1-x}Bi_xCrO_3$ compound based on its multiferroic properties.

Despite the interesting properties of $La_{1-x}Bi_xCrO_3$, the origin of its ferroelectricity has not been yet firmly established. In fact, there is not any detailed discussion on the multiferroic properties of $La_{1-x}Bi_xCrO_3$ based on first-principles calculations in the literature. For this reason, in this work we employ density functional theory (DFT) + Hubbard potential (U) formalism to theoretically study structural properties, electronic structure, chemical bonding, and magnetism. Additionally, the ferroelectric properties of $La_{1-x}Bi_xCrO_3$ are addressed using the Modern Theory of Polarization via Berry phase approach. Finally, a comparative analysis is presented between reported experimental results and the theoretical calculations in this work.

2. Computational details

First-principles calculations were performed using DFT as implemented in the Quantum-Espresso package [9]. Norm-conserving pseudopotentials were generated with the OPIUM package [10-11] and the generalized gradient approximation (GGA) based on the Perdew-Burke-Ernzerhof (PBE) functional was used for exchange-correlation effects. For a correct description of the pseudopotentials, 15 valence electrons were selected for Bi ($5d^{10}6s^26p^3$), 11 for La ($5s^25p^65d^16s^2$), 14 for Cr ($3s^23p^63d^44s^2$) and 6 for O ($2s^22p^4$). A plane-wave energy cutoff of 55 Ry was used throughout the calculations. All atomic positions and lattice constants were optimized until the magnitude of the residual energy and force acting on each atom was smaller than 10^{-4} Ry/atom and 10^{-3} Ry/au, respectively. The Monkhorst-Pack k-point 3×3×2 and 6×6×4 meshes were used for geometry optimization and electronic structure calculations, respectively. Taking into account the strong Coulomb repulsion between the localized d-states of Cr, we used the GGA + Hubbard potential (U) to describe the correlation effects in transition metal oxides. For this work, the optimal value of U applied on Cr was 5 eV, which ensures a magnitude of magnetization and bandgap similar to those experimentally reported (see below). For the magnetic moments calculation, the spin-orbit interaction has been considered.

The polarization of LCO and $La_{0.75}Bi_{0.25}CrO_3$ (BLCO) were calculated via Berry phase using the method first developed by King-Smith and Vanderbilt [12-13]. In this theory, the total polarization can be expressed as

$$\boldsymbol{P} = \boldsymbol{P}_{ion} + \boldsymbol{P}_{el}$$

where

$$\boldsymbol{P}_{ion} = \frac{e}{\Omega}\sum_s Z_s^{ion}\,\boldsymbol{r}_s$$

where $\boldsymbol{P}_{ion}$ is the classical ionic contribution in the unit cell volume Ω, arising from positive point charges eZ_s^{ion} located at atomic positions $\boldsymbol{r}_s$. The electronic contribution $\boldsymbol{P}_{el} = \sum_n^{occ} \boldsymbol{P}_n$ in the discrete *k*-space is computed using the Berry phase formalism where the $\boldsymbol{P}_n$ contribution to $\boldsymbol{P}_{el}$ from band *n* is given by

$$\boldsymbol{P}_n = \frac{1}{2\pi}\frac{e}{\Omega}\sum_j \varphi_{n,j}\,\boldsymbol{R}_j$$

$$\varphi_{n,j} = \Omega_{BZ}^{-1} \int_{BZ} d^3\, k \langle u_{n\boldsymbol{k}} | -i\boldsymbol{G}_j \cdot \nabla_{\boldsymbol{k}} | u_{n\boldsymbol{k}} \rangle$$

where $\boldsymbol{R}_j$ is the real-space primitive lattice vector corresponding to the primitive reciprocal lattice vector $\boldsymbol{G}_j$ in direction j. $\Omega_{BZ} = (2\pi)^3/\Omega$ is the Brillouin zone (BZ) volume. The $\varphi_{n,j}$ is the Berry phase for band *n* for a given direction j.[14]

Because of the Born–von Kármán periodic boundary conditions, there is an ambiguity in the choice of unit cell and the total polarization may only be determined up to an integer multiple of the polarization quantum $e\boldsymbol{R}/\Omega$, where *e* is the charge of the electron, $\boldsymbol{R}$ is a lattice vector in the direction of polarization, and Ω is the volume of the unit cell.[12-15]

3. Results and discussion

The LCO orthorhombic perovskite unit cell (space group # 62 Pbnm), is illustrated in figure 1(a) where the lattice parameters *a = 5.5140 Å*, *b = 5.4780 Å* and *c = 7.7520 Å*, and the Wyckoff positions of La *4c* (0.9923, 0.0156, 0.2500), Cr *4b* (0.0000, 0.5000, 0.0000), O *8d* (0.7264, 0.2746, 0.0334) and O *4c* (0.0675, 0.4837, 0.2500) taken from the COD file # 1533275. The LCO has 20 atoms in the unit cell (4 La, 4 Cr and 12 O). figure 1(b) shows the unit cell of the LCO doped with 25% of Bi ($La_{0.75}Bi_{0.25}CrO_3$) (BLCO) that is within the degree of impurification studied in reference 4; fortunately, this concentration allows us to work with unit cells with a small number of atoms, thus facilitating the DFT calculations.

After structural relaxation, the lattice parameters, bond distances and angles (Cr-O-Cr) for both LCO and BLCO systems are reported in table 1. The lattice parameters obtained for LCO are similar to those reported in other works [1, 16-17]. Since the polar vector is along the face diagonal of the orthorhombic unit cell, we analyze the displacement of the ions on the $(\bar{1}00)$ plane (see figure 1(c) and 1(d)), and $(0\bar{1}0)$ (see figure 1(e) and 1(f)) for LCO and BLCO systems (see table 1). For the $(\bar{1}00)$ plane for LCO (figure 1(c)) and BLCO (figure 1(d)) systems, the distance of Cr4-Bi5 and Cr4-La4 of the BLCO increases up to ~ 0.07 Å with respect to the separation between Cr4-La5 y Cr4-La4 of the LCO, while the distance between Cr4-Bi1 and Cr4-La6 of the BLCO is practically maintained unchanged when compared to the separation between Cr4-La1 and Cr4-La6 of the LCO.

Similarly, on the $(0\bar{1}0)$ plane (figure 1(e) for LCO and 1(f) for BLCO), the distance between Cr1-La2 and Cr1-La4 of the BLCO increases, while the Cr1-La1 and Cr-La3 interval of the BLCO remains equal compared to the LCO (see table 1). On the other hand, the distance between Cr1-Cr2, Cr1-Cr3 (figure 1f) and Cr4-Cr5, Cr4-Cr6 (figure 1d) increases from ~3.91 Å to ~3.95 Å when the LCO is doped with 25% of Bi. The displacement of the ions in the BLCO produces an increase in the volume of the unit cell from 241.2698 Å3 for the LCO to 248.6957 Å3 for the BLCO. Such volume increase together with the displacement of the ions could produce the experimentally-observed ferroelectric behavior. [4,8]

In a comparative analysis of energy between different non-magnetic (NM), ferromagnetic (FM) and G-type antiferromagnetic (AFM-G) arrangements for both LCO and BLCO (table 1), it has been shown that the lowest-energy electronic configuration of LCO corresponds to the AFM-G ordering, in agreement with the experimental results reported in reference 1. On the other hand, BLCO is energetically more stable with the FM ordering (see table 1). Our results agree with the experimental observation that the magnetic properties of BLCO are different compared with those of LCO.[8] At the same time, the Cr-O-Cr angles are similar to those reported by reference 16. The Cr-O-Cr angle of BLCO is lower than that of LCO (table 1), indicating the strong distortion of the CrO_6 octahedra in the BLCO compared with the LCO. In fact, our results are in good correspondence with the appearance of FM in $BiFeO_3$ clusters with the decreasing of the Fe-O-Fe angle value.[18] The strong distortion of octahedra, in turn, is due to the stereochemically active lone pair electrons of the Bi^{3+}.[4] Note that the ionic radii of La^{3+} (1.30) and Bi^{3+} (1.31) in coordination VIII are quite similar.[19] Considering the AFM-G ordering of LCO and the spin orbit coupling, the value of the magnetic moment of Cr ion is 2.594 μB, which is in good agreement with the experimental reported value of 2.8 μB [1].

For the BLFO case, in turn, taking into account the FM ordering and the spin orbit coupling, a decrease of the magnetic moment for the Cr ion is observed (the computed value is 2.533 μB) which can be associated with the strong interaction with the oxygen ions.

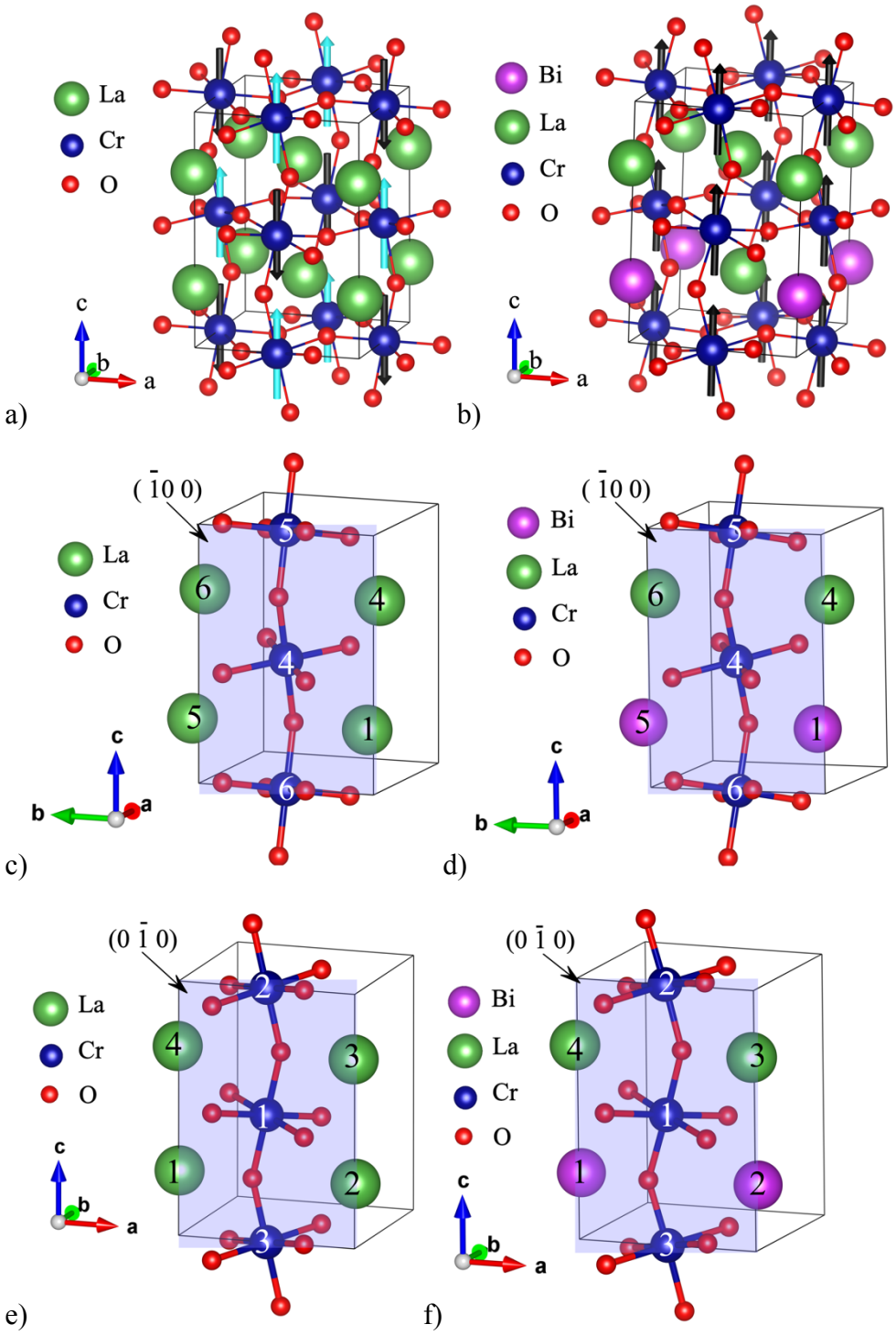

Figure 1. (Color online) Unit cell of (a) LCO and (b) BLCO after structural relaxation; the presentation of the ions on the ($\bar{1}$00) plane for (c) LCO and (d) BLCO; the presentation of the ions on the (0$\bar{1}$0) plane for (e) LCO y (f) BLCO.

Table 1. Optimized lattice parameters, distance between the cations A (Bi, La) and B (Cr) of the perovskite type structure (unit Å), angles (°), system energy (eV) and magnetic moment μ (μB per atom) for LCO and BLCO in bulk.

	LCO	BLCO
a	5.5693	5.6259
b	5.5329	5.5891
c	7.8297	7.9093
V(Å^3)	241.2698	248.6957
$(0\bar{1}0)$ plane		
Cr1-Bi1 (La3)		3.4372 (3.4617)
Cr1-Bi2 (La4)		3.4536 (3.4293)
Cr1-La1 (La3)	3.4343 (3.4343)	
Cr1-La2 (La4)	3.3835 (3.3835)	
Cr1-Cr2 (Cr3)	3.9149 (3.9149)	3.9515 (3.9578)
$(\bar{1}00)$ plane		
Cr4-Bi5 (La4)		3.6086 (3.6086)
Cr4-Bi1 (La6)		3.2505 (3.2423)
Cr4-La5 (La4)	3.5423 (3.5423)	
Cr4-La1 (La6)	3.2393 (3.2393)	
Cr4-Cr5 (Cr6)	3.9149 (3.9149)	3.9533 (3.9559)
Cr-O	2.0042	2.0490
Cr-O-Cr (°) (along c)	155.30	150.08
Cr-O-Cr (°) ((001) plane)	156.55	149.36
NM (eV)	0.0000	0.0000
FM (eV)	-14.5843	-13.3277
AFM-G (eV)	-14.7092	-13.3260
μ_{Cr}	2.594	2.533
μ_{La}	0.000	0.009
μ_{Bi}	--	0.004
μ_O	0.001	0.056

To better understand the significance of the calculated structural results, we will now analyze the band structure and the density of states (DOS) of both LCO and BLCO systems. figure 2(a) and 2(b) present the band structure for the spin-up and spin-down states and the total density of states (TDOS) of the LCO and BLCO systems, respectively. The value of the Fermi energy (EF) is set to zero. In the LCO system (figure 2(a)) no differences are distinguished between the spin-up and spin-down bands and the TDOS is completely symmetric in correspondence with the AFM-G arrangement of the Cr^{3+} magnetic moments. The value of the electronic gap was 3.1 eV for the direct bandgap and 3.0 eV for the indirect bandgap, close to that experimentally reported of 3.4 eV [20]. As expected, in the case of the BLCO, the TDOS distribution (figure 2(b)) is not symmetric for spin-up and spin-down states. The spin-up and spin-down states are characterized by the direct bandgap of 1.7 eV and 4.3 eV, and an indirect bandgap of 1.0 eV and 3.6 eV, respectively. Such complex band structures, allow predicting that the FM-BLCO has potential applications in Spintronics as magnetic semiconductor.

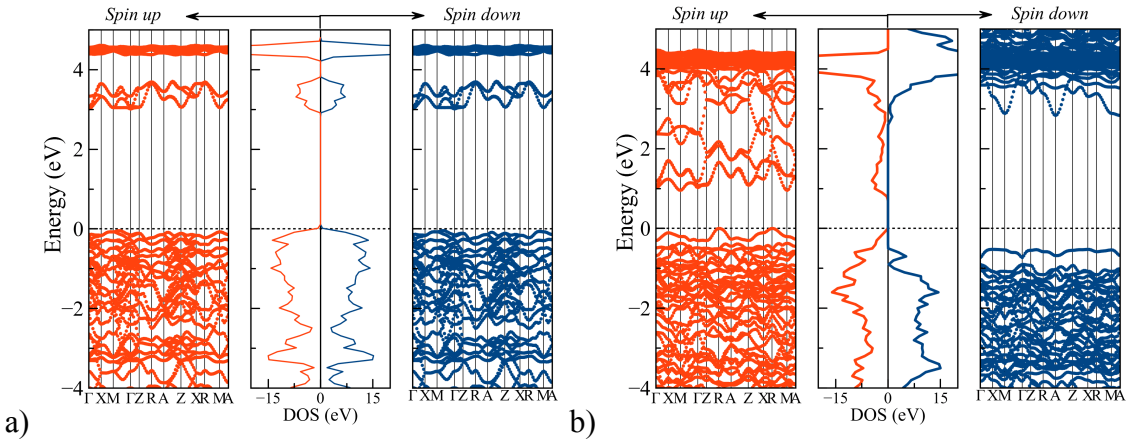

Figure 2. (Color online) Band structure and TDOS (in the center part of the figure) obtained for (a) LCO and (b) BLCO system.

Figure 3 shows the selected partial density of states (PDOS) for the LCO (figure 3(a)) and BLCO (figure 3(c), respectively. For the LCO case, figure 3(a), it is observed that the states of the La-5*d* orbitals are mainly in the valence band (VB) below EF. Meanwhile, as expected for the states of La-4*f*, they contribute mainly at a higher level in the conduction band above EF. However, near below EF, the participation of the La-5*d* and La-4*f* states is practically negligible. On the other hand, a strong hybridization is observed between the Cr-3*d* and O-2*p* orbitals along of all energy ranges indicating the existence of a certain degree of covalence of the Cr-O bonds. Moreover, as shown in the PDOS of Cr-3*d* and O-2*p* (see figure 3(c)), the highest occupied molecular orbitals (HOMO level) near below EF are dominated by Cr-t_{2g} orbitals and O-2*p*, respectively. Here, the HOMO level is dominated by the states of the O-2*p*, Cr-3*d* while the minimum of the conduction band (LUMO level) is mainly dominated by the Cr-3*d* states. With this, the energy of the bandgap is established by the states of the O-2*p* in the VB and the states of Cr-3*d* in the CB for LCO. Thus, the AFM-G ordering can be explained by superexchange interactions between the Cr ions mediated by the oxygen ions between them. [21-22] As expected in the case of the BLCO, the PDOS analysis shows that the La-5*d*, La-4*f* and Bi-6*p* states contribution is practically zero near below EF (figure 3(b)). Different to the LCO, the results of PDOS for the BLCO indicate that the bandgap is established by the O-2*p*, Bi-6*s* and Cr-3*d* states near below EF and Cr-3*d* in the CB. The Bi-6*s* electrons of the lone-pair are found in the range of -10 eV to -9.5 eV and with lower presence near below EF, converting them into localized electrons able to produce ferroelectric polarization.[23] Moreover, a strong hybridization between the Cr-3*d* and O-2*p* states is at all energy ranges in VB (figure 3(b)), and particularly near below EF is dominated for the spin-up t_{2g} (figure 3(d)) orbital of Cr and O-2*p* exhibiting a higher degree of covalence in the Cr-O bonds that, additionally, allow mixed valence of the Cr ions. This result can be associated to the higher distortion of the CrO_6 octahedron for BLCO which increases the separation of the degenerate Cr-t_{2g} and Cr-*eg* orbitals energy and reduce the energy gap between the CB and VB.[22,24] Thus, the ferromagnetic ordering can be explained by superexchange or double-exchange interactions between the Cr ions mediated by the oxygen ions between them.[21-22]

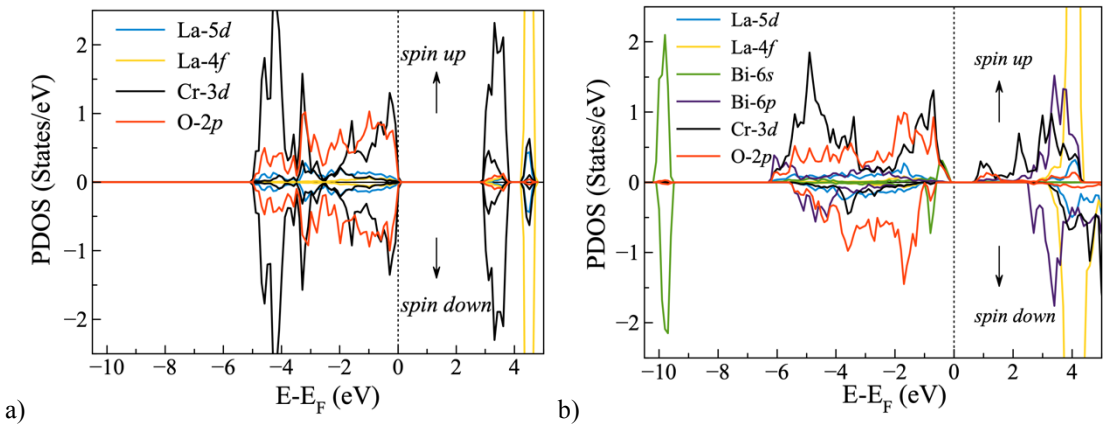

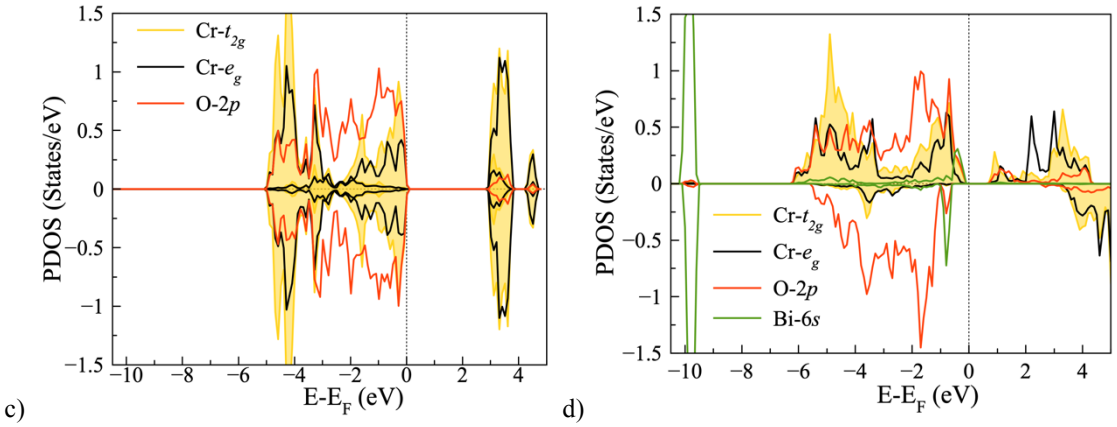

Figure 3. (Color online) Selected PDOS for (a) LCO and (b) BLCO bulk. PDOS of Cr-t_{2g} and Cr-e_g, O-2p and Bi-6s for (c) LCO and (d) BLCO.

Figure 4(a) and 4(b) show the electronic density (ED) and electron localization function (ELF) projected on the $(\bar{1}00)$ plane for the LCO, respectively, where it can be seen that a small charge density is shared between the ions of O and Cr. The directional nature of the shared charge distribution between the ions of O and Cr confirms the presence of covalence in the Cr-O bonds as discussed previously in the PDOS analysis in figure 3(a). On the other hand, it is observed that the electron density of the La^{3+} and the O^{2-} ions, barely overlap, indicating a purely ionic bond.

Figure 5(a) and 5(b) show the ED and ELF projected on the $(\bar{1}00)$ plane for the BLCO. Similar to what happens in LCO, the charge density shared between the O^{2-} ion with the Bi^{3+}, La^{3+} ions barely overlap, which entails to an mainly ionic bond. A directional nature of the charge distribution between the ions of Cr and O is observed, confirming the covalent character of the Cr-O bonds. From another point of view, the ELF is asymmetric around the Bi^{3+} ions as result of the Bi-6s lone pair presence. Such asymmetric distribution of the lone-pair charge leads to a structural distortion that gives rise to the spontaneous polarization (**P**s).[23] figure 6(a) and 6(b), describe the molecular orbital (MO) projected on the $(\bar{1}00)$ plane corresponding to the Cr-3d, O-2p, La-5d and Bi-6s orbitals in EF for the LCO and BLCO, respectively. It is possible to identify the presence of a non-uniform charge distribution corresponding to Bi^{3+} ascribed, specifically, to the Bi-6s lone-pair in the BLCO.

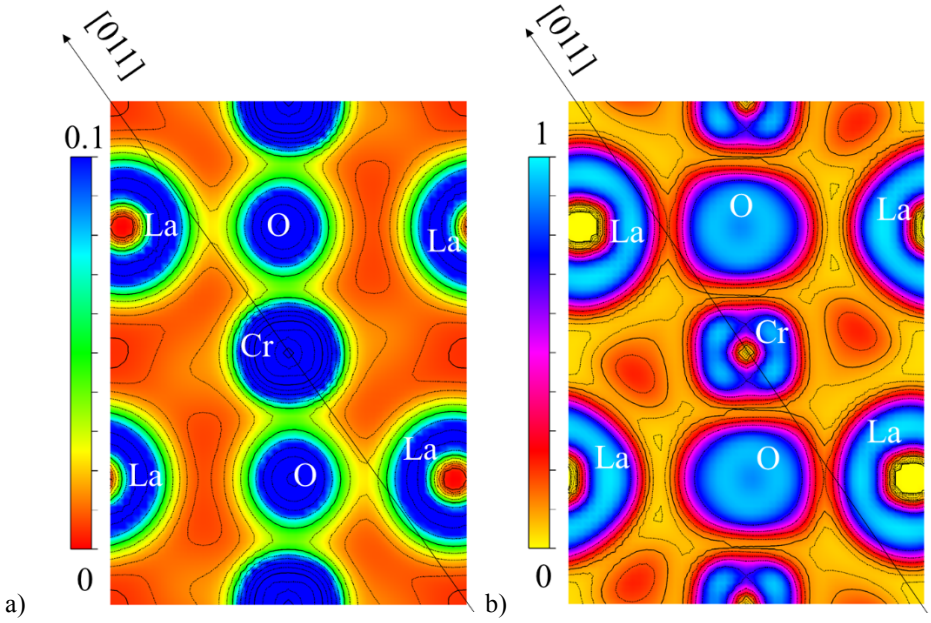

Figure 4. (Color online) (a) Electronic density and (b) ELF projected on the $(\bar{1}00)$ plane for the LCO.

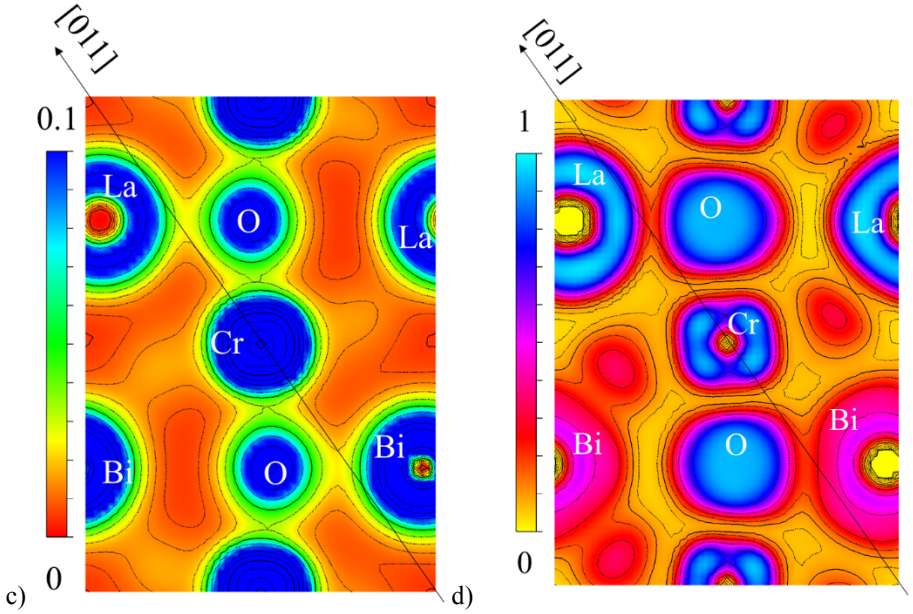

Figure 5. (Color online) (a) Electronic density and (b) ELF projected on the ($\bar{1}$00) plane for the BLCO.

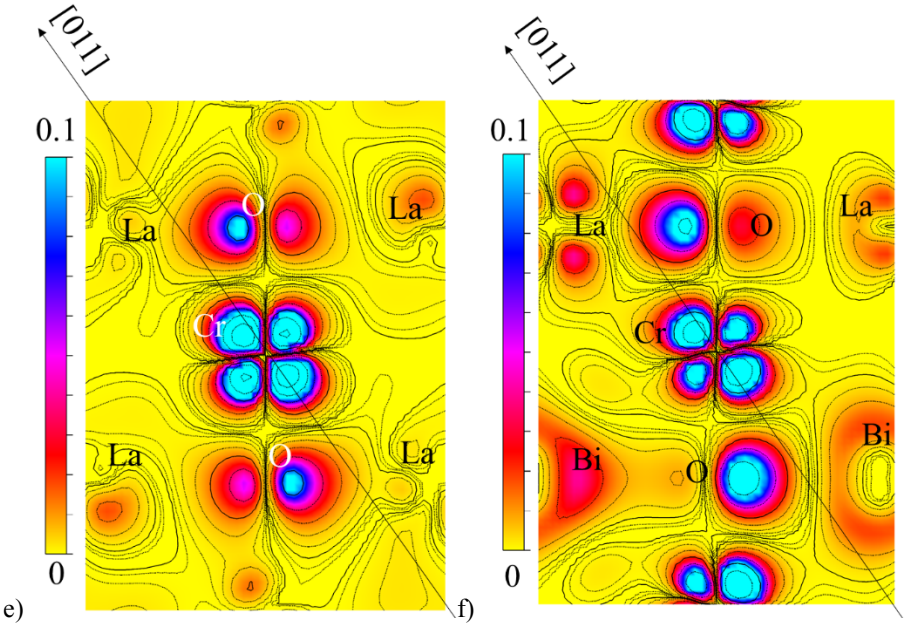

Figure 6. (color online) The molecular orbital (MO) images projected on the ($\bar{1}$00) plane for (a) LCO and (b) BLCO in Fermi level.

The minimum values of the polarization lattice ($\mathbf{P}_{min}$)[18], and the values of the polarization quantum ($e\boldsymbol{R}/\Omega$) along the lattice vector for LCO and BLCO are reported in table 2. For the LCO system, $\mathbf{P}_{min}$ is zero along each direction of the lattice parameters, this result coincides with the non-ferroelectric observations of the LCO.[17] For the BLCO system, a contribution of polarization is observed in the [010] and [001] direction, resulting in a net polarization of 30.41 + 62.35 μC/cm^2 in the [011] direction, where 62.35 μC/cm^2 is the polarization quantum along [011]. To calculate **P**s of BLCO, we use the centrosymmetric orthorhombic unit cell (space group #62 Pbnm) of LCO, taken from the COD file # 1533275, as a reference cell (λ = 0)[14], the polarization for the centrosymmetric structure of LCO is of 32.45 μC/cm2 along the [011] direction, which is half a polarization quantum [14] (see table 2). Finally, the $\mathbf{P}_S$ of BLCO is evaluated as the difference in polarization between the centrosymmetric structure (λ = 0) and the distorted structure (λ = 1) of BLCO. Therefore, in our work, we obtained a $\mathbf{P}_S$ for BLCO of 60.31 μC/cm2, evincing the possibility and compatibility of FE and FM orderings coexistence in the Bi doped LCO compound. This result opens up the possibility of applications for BLCO based on its multiferroic properties.

Table 2. Minimum value of the polarization lattice ($\mathbf{P}_{min}$), the polarization quantum $|e\mathbf{R}/\Omega|$ in μC/cm^2 calculated by the modern theory of polarization.

	Direction	$\mathbf{P}_{min}$	$\lvert e\boldsymbol{R}/\Omega\rvert$
LCO	[100]	0.00	36.96
	[010]	0.00	36.71
	[001]	0.00	51.96
BLCO	[100]	2.41	36.21
	[010]	20.68	35.98
	[001]	22.30	50.92
	[011]	30.41	62.35
LCO COD#1533275	[011]	0.00	64.90

4. Conclusion

Using the DFT+U formalism, we have successfully studied the multiferroic properties of LCO bulk doped Bi with *Pbnm* symmetry. We have observed that the $LaCrO_3$ is stable under an AFM-G-type configuration, while $La_{0.75}Bi_{0.25}CrO_3$ is found stable in the FM configuration. This is due to the decrease of the Cr-O-Cr angle which is strongly related with the high degree of covalence of the spin-up Cr-t_{2g} and O-2*p* orbitals in the Cr-O bonds. On the other hand, the $\mathbf{P}_S$ value calculated via Berry phase for pure $LaCrO_3$ is zero, while a $\mathbf{P}_S$ for $La_{0.75}Bi_{0.25}CrO_3$ of 60.31 μC/cm^2 in [011] direction is predicted, and is attributed to the displacements of the ions caused by the Bi lone pair. The results obtained in this theoretical study are consistent with the reported experimental results in the literature and, in addition, allow to establish the origin of ferroelectricity observed experimentally in BLCO.

Acknowledgements

This work was partially supported by DGAPA-UNAM Proj. IN105317. The autor thank DGTIC-UNAM for computer support through Project LANDCAD-UNAM-DGTIC-348. E. Martínez-Aguilar thanks CoNaCyt for Scholarship Grant 290934 and H´Linh H´Mõk thanks CoNaCyt for Scholarship Grant 290784.

References

[1] Koehler W C and Wollan E O 1957 *J. Phys. Chem. Solids*, **2** 100-106.
[2] Baukal W, Kuhn W, Kleinschmager H, Rohr F J 1976–1977 *J. Power Sources* **1** 203–213.
[3] Feduska W, Isenberg A O 1983 *J. Power Sources* **10** 89–102.
[4] Chen J I L, Mahesh Kumar M, and Ye Z-G 2004 A new ferroelectric solid solution system of $LaCrO_3$–$BiCrO_3$ *J. Solid State Chem.* **177** 1501-1507.
[5] Sakai N, Fjellvag H, and Hauback B C 1996 Structural, magnetic, and thermal properties of $La_{1-t}Ca_tCrO_{3-\delta}$. *J. Solid State Chem.* **121** 202-213.
[6] Tezuka K and Hinatsu Y 1998 Magnetic and neutron diffraction study on perovskites $La_{1-x}Sr_xCrO_3$. *J. Solid State Chem.* **141** 404-410.
[7] Chakraborty K R, Yusuf S M, Krishna P S R, Ramanadham M and Tyagi A K 2004 Low-temperature neutron diffraction study of $La_{0.95}Nd_{0.05}CrO_3$. *Pramana - J Phys* **63** 251-255.
[8] Guo H-Y, Chen J I L and Ye Z-G 2007 *J Mater. Res*, **22** 8 2081-2086.
[9] Paolo Giannozzi *et al* 2009 *J. Phys.: Condens. Matter* **21** 395502.
[10] Rappe A M, Rabe K M, Kaxiras E and Joannopoulos J D 1990 *Phys. Rev. B* **41** 1227.
[11] Ramer N J and Rappe A M 1999 *Phys. Rev. B* **59** 12471-12478.
[12] King-Smith R D and Vanderbilt D 1993 *Phys. Rev. B* **47** 1651-1654.
[13] Vanderbilt D and King-Smith R D 1993 *Phys. Rev. B* **48** 4442-4455.
[14] Resta R and Vanderbilt D, 2007 *Topics Appl. Physics* **105** 31-68.
[15] Neaton J B, Ederer C, Waghmare U V, Spaldin N A and Rabe K M 2005 *Phys. Rev. B* **71** 014113.

[16] Takuya Okugawa *et al* 2018 *J. Phys Condens. Matter* **30** 075502
[17] Yoshii K, Ikeda N, Shimojo Y, Ishii Y 2017 *Materials Chemistry and Physics* **190** 96-101
[18] Modak P, Lahiri D and Sharma S M 2016 *J. Phys. Chem. C* **120** 8411-8416
[19] Shannon R D 1976 *Acta Cryst*, Sect. A **32** 751-767
[20] Arima T, Tokura Y and Torrance J B 1993 *Phys. Rev. B* **48** 17006
[21] Goodenough J B and Loeb A L 1955 *Phys. Rev* **98** 564
[22] Blundell S 2001 *Magnetism in Condensed Matter* Oxford University Press
[23] Hill N A, Battig P and Daul C 2002 First principles search for multiferroism in $BiCrO_3$ *J. Phys. Chem. B* **106** 3383-3388.
[24] Wolfram T and Ellialtioglu S 2006 *Electronic and Optical Properties of D-Band Perovskites* Cambridge University Press